

Fig. 5. Characterization of Enhanced LIGO interferometer as a squeezing detector. Red points show measured squeezing and anti squeezing between 1.9 kHz and 3.7 kHz. Blue trace is a fit to the red points with $\eta = 38 \pm 3\%$ and $\bar{\theta} = 81 \pm 6$ mrad. Control bandwidths were consistent for measurements at different nonlinear gains. The black and green points were measured at a later date with $\eta = 42 \pm 7\%$. After measurement of the black point ($\bar{\theta} = 109 \pm 9$ mrad), the interferometer alignment was adjusted slightly and the squeezing angle lock point adjusted, reducing the quadrature fluctuations to ($\bar{\theta} = 37 \pm 6$ mrad) as shown by the green point.

Table 1. Summary of contributions to total relative quadrature fluctuations (mrad RMS) and independent measurements made at high nonlinear gains.

Source		Estimate	Measurement
Squeezer	OPO length noise	24.6 ± 3	
	Coherent locking field(CLF) sensor noise	1.8 ± 0.5	
	OPO and SHG length control sidebands	< 1	
	Crystal temperature fluctuations	unknown	
Total intrinsic to squeezer		24.7 ± 2	21 ± 6
IFO	Interferometer (IFO) sidebands	3.1 ± 0.4	
	Alignment jitter coupling (inferred from total)	35-100	
Squeezer + IFO total (good alignment)			37 ± 6

considered here that cause quadrature fluctuations, and our estimates and measurements of their contribution to the total in our experiment. The dominant mechanism for relative fluctuations between the squeezed and measured quadrature in our experiment was lock point errors introduced by alignment fluctuations, closely followed by length fluctuations of the OPO. Other smaller contributions were phase noise of the second harmonic pump, temperature fluctuations, sensor electronics and shot noise imposed by our control scheme, and phase noise of the local oscillator.

In the early stages of Advanced LIGO [29], the total effective losses are expected to be reduced to 20-28%, mainly due to improvements in OMC transmission and mode matching. This means that a reduction of the quadrature fluctuations to 5-15 mrad would allow for confident

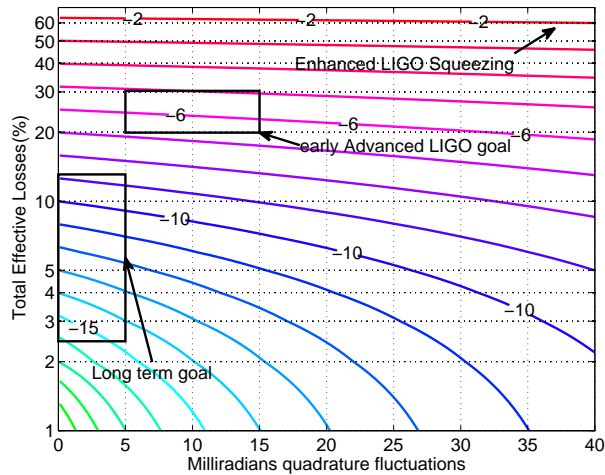


Fig. 6. Squeezing targets for gravitational wave detectors, in decibels relative to shot noise. This experiment measured -2.1 dB of squeezing in Enhanced LIGO, with 55% losses and at least 37 ± 6 mrad squeezing angle fluctuations. For Advanced LIGO we would like to be able to measure at least -6 dB of squeezing in an initial implementation. Since the total losses are expected to be 20-28%, planning for 15 mrad or less of phase noise would allow for -6 dB of squeezing. Designs for third generation detectors call for even higher levels of squeezing [31], which will place very stringent limits on the total quadrature fluctuations and losses.

planning for -6 dB of noise reduction due to squeezing, as shown by the rectangle in Fig. 6. These levels of quadrature fluctuations have already been demonstrated with both traveling wave and standing wave OPO designs [11, 30]. Third generation detectors seek to implement 10 dB or more of squeezing [31], placing very stringent requirements on both optical losses and quadrature fluctuations.

The performance of the coherent quadrature control schemes is limited by lock point errors introduced by alignment jitter, OPO length fluctuations, and crystal temperature fluctuations. The bandwidth of the coherent control scheme is limited by arm cavity resonances in an interferometer with Fabry-Perot arms; in LIGO this limits the bandwidth to around 10 kHz. Quantum noise locking [32] is an alternative to coherent locking that is immune to lock point errors and could potentially reduce the quadrature fluctuations to a comfortable level for Advanced LIGO when used in combination with a coherent lock [7]. However, the dither of the quadrature angle required to produce a noise locking error signal will need to be small compared to the acceptable level of quadrature fluctuations, meaning that this technique will have a small signal to noise ratio and therefore low bandwidth. Ultimately, to achieve the low levels of quadrature fluctuations needed, the lock point errors of the coherent control scheme need to be addressed.

One option is to derive the coherent control error signal in transmission of the OMC [7], which should eliminate the alignment coupling to the quadrature angle by filtering the higher order modes. The OPO may be mounted on a seismic isolation platform inside the vacuum system in order to meet the requirements for scattered light noise. This will have the benefit of reducing both the length fluctuations of the OPO and relative alignment fluctuations between the OPO and the interferometer, mitigating both of the dominant sources of quadrature fluctuations in this experiment. Intensity stabilization of the second harmonic pump [27], or a direct readout of the crystal temperature similar to the scheme used in [26], may help to mitigate lock

point errors caused by crystal temperature fluctuations.

We have shown that careful attention must be paid to each of the major causes of quadrature fluctuations in order to reach high levels of squeezing enhancement in a gravitational wave interferometer, or any experiment where high levels of squeezing are needed. The low frequency noise requirements of a gravitational wave detector preclude use of a coherent field at the carrier frequency for sensing and control of the quadrature angle, making it necessary to use either incoherent “noise” locking or coherent control schemes with a frequency-shifted sideband. Both of these techniques have limitations: the coherent locking technique introduces lock point errors due to misalignment, OPO length changes and crystal temperature fluctuations, while noise locking relies on a dither of the quadrature angle. Ultimately, quadrature fluctuations need to be mitigated at the source rather than suppressed by high bandwidth feedback. This requires careful planning and an understanding of each of the sources of quadrature fluctuations.

6. Appendix 1: Calculation of squeezed quadrature angle in an OPO including detunings and imperfect phase matching

The Hamiltonian for an OPO without losses is:

$$H = \hbar 2\omega b^\dagger b + \hbar \omega a^\dagger a + \frac{i\hbar}{2} (\varepsilon a^{\dagger 2} b + \varepsilon^* a^2 b^\dagger) \quad (8)$$

where a, a^\dagger are annihilation and creation operators for the fundamental field at the interferometer carrier frequency ω written in the rotating frame at that frequency, b, b^\dagger are operators for the second harmonic field in the rotating frame at 2ω , and ε is the nonlinear coupling parameter which is real when the crystal temperature is exactly tuned for phase matching. We can calculate the spectrum of squeezing at the output of the OPO using the quantum Langevin equations and introducing two losses to the cavity, one representing all of the intracavity losses and absorption and another representing transmission through the front coupler [24, 25]. The steady state solution to the cavity equation of motion for the second harmonic field in the parametric approximation is:

$$b = \frac{\sqrt{2\gamma_b^f} |B_{in}| e^{i\theta_B}}{\gamma_b^{\text{tot}} (1 - i\Delta_b/\gamma_b^{\text{tot}})} \quad (9)$$

where $B_{in} = |B_{in}| e^{i\theta_B}$ is the incident second harmonic pump field in the rotating frame at 2ω , γ_b^f is the field decay rate of the front coupler for the second harmonic field, γ_b^{tot} is the total field cavity decay rate for the second harmonic field, and Δ_b is a detuning of the second harmonic field from the cavity resonance. The operators can be separated into constant and time dependent parts, ($a = \bar{a} + \delta a(t), b = \bar{b} + \delta b(t)$), and the equations of motion for the fundamental field linearized by dropping terms that are the product of two fluctuating components. To avoid noise couplings that mask low frequency squeezing, there should be no circulating coherent field at the fundamental frequency so $\bar{a} = 0$ [22]. The equations of motion for the fundamental field annihilation and creation operators are given in matrix form by:

$$\delta \dot{\mathbf{a}} = \gamma_a^{\text{tot}} \mathbf{M} \delta \mathbf{a} + \sqrt{2\gamma_a^f} \delta \mathbf{A}_{1,\text{in}} + \sqrt{2\gamma_a^f} \delta \mathbf{A}_{f,\text{in}} \quad (10)$$

where

$$\delta \mathbf{a} = \begin{pmatrix} \delta a \\ \delta a^\dagger \end{pmatrix}, \quad \mathbf{M} = \begin{pmatrix} -1 + i \frac{\Delta_a}{\gamma_a^{\text{tot}}} & x \frac{e^{i\theta_B}}{1 - i\Delta_b/\gamma_b^{\text{tot}}} \\ x^* \frac{e^{-i\theta_B}}{1 + i\Delta_b/\gamma_b^{\text{tot}}} & -1 - i \frac{\Delta_a}{\gamma_a^{\text{tot}}} \end{pmatrix}, \quad x = \frac{\sqrt{2\gamma_b^f} |B_{in}|}{\gamma_b^{\text{tot}}} \frac{\varepsilon}{\gamma_a^{\text{tot}}} \quad (11)$$

and $\delta\mathbf{A}_{1,\text{in}}$ is a vector of the annihilation and creation operator for the vacuum fluctuations that leak into the cavity through intra-cavity losses and $\delta\mathbf{A}_{f,\text{in}}$ are the vacuum fluctuations incident on the front coupler of the OPO, $\gamma_a^{\text{tot}} = \gamma_a^l + \gamma_a^f$ is the total cavity field decay rate for the fundamental field, γ_a^f is the decay rate for the front coupler for the fundamental field, γ_a^l is the decay rate due to intracavity losses, and Δ_a is the cavity detuning at the fundamental frequency. The normalized nonlinear coupling x is real when the temperature is tuned to phase matching, and reaches unity when the OPO reaches the threshold for spontaneous parametric down conversion. Moving into the frequency domain:

$$\delta\tilde{\mathbf{a}}(\Omega) = (\Omega - \gamma_a^{\text{tot}}\mathbf{M})^{-1} \left[\sqrt{2\gamma_a^l}\delta\tilde{\mathbf{A}}_{1,\text{in}}(\Omega) + \sqrt{2\gamma_a^f}\delta\tilde{\mathbf{A}}_{f,\text{in}}(\Omega) \right] \quad (12)$$

Here we have assumed that \mathbf{M} does not depend on time, which is a good approximation when the time dependence is at frequencies much smaller than the cavity linewidths $\gamma_b^{\text{tot}}, \gamma_a^{\text{tot}}$, as temperature and length fluctuations will be. Using the input output relations [24]:

$$\begin{aligned} \delta\mathbf{A}_{f,\text{out}}(\Omega) &= \sqrt{2\gamma_a^f}\delta\tilde{\mathbf{a}}(\Omega) - \delta\tilde{\mathbf{A}}_{f,\text{in}}(\Omega) \\ &= \left(2\gamma_a^f (i\Omega\mathbf{I} - \gamma_a^{\text{tot}}\mathbf{M})^{-1} - \mathbf{I} \right) \delta\mathbf{A}_{f,\text{in}}(\Omega) + 2\sqrt{\gamma_a^l\gamma_a^f} (i\Omega\mathbf{I} - \gamma_a^{\text{tot}}\mathbf{M})^{-1} \delta\mathbf{A}_{1,\text{in}}(\Omega) \end{aligned} \quad (13)$$

When the measurement frequency Ω is small compared to the optical frequency ω , the quadrature operators of the output field are given in terms of the annihilation and creation operators by [33]:

$$\delta\tilde{\mathbf{X}}_{f,\text{out}}(\Omega) = \begin{pmatrix} \delta\tilde{X}_1(\Omega) \\ \delta\tilde{X}_2(\Omega) \end{pmatrix} = \begin{pmatrix} 1 & 1 \\ -i & i \end{pmatrix} \delta\tilde{\mathbf{A}}_{f,\text{out}}(\Omega) = \mathbf{R}\delta\tilde{\mathbf{A}}_{f,\text{out}}(\Omega) \quad (14)$$

Using the fact that the incident vacuum fluctuations are uncorrelated [34], the variance of the output field ($V_1 = |\delta\tilde{X}_1|^2$) can be calculated using Eqs. (11), (13), and (14); results are plotted in Fig. 3. The usual equations for the variance of the output field can be found by setting the detunings Δ_a, Δ_b to zero, assuming that ε is real:

$$\begin{aligned} V_1(\theta_b, \Omega) &= V_+(\Omega) \cos^2(\theta_b/2) + V_-(\Omega) \sin^2(\theta_b/2) \\ V_{\pm} &= 1 \pm \frac{4\eta_{\text{esc}}x}{(1 \mp x)^2 + (\Omega/\gamma_a^{\text{tot}})^2} \end{aligned} \quad (15)$$

where $\eta_{\text{esc}} = \gamma_a^f/\gamma_a^{\text{tot}}$ is the escape efficiency. By propagating this field to the detector and taking into account additional losses in propagation, homodyne efficiency and photo-diode efficiency, Eq. (1) is obtained.

7. Appendix 2: Calculation of control signals including detunings and imperfect phase matching

To calculate the error signal produced by the coherent locking technique, we can use the cavity equations of motion for a non-degenerate OPO, approximating the two coherent control sidebands as separate modes of the cavity, called the signal (a_s) and idler (a_i). Assuming that the signal and idler fields are small compared to the second harmonic field the parametric approximation holds and the second harmonic field is described by Eq. (9). Ignoring quantum fluctuations, the equations of motion are:

$$\dot{a}_s = (i\Delta_s - \gamma_a^{\text{tot}})a_s + \varepsilon b a_i^\dagger + \sqrt{2\gamma_a^c} A_{s,\text{in}} \quad (16)$$

$$\dot{a}_i = (i\Delta_i - \gamma_a^{\text{tot}})a_i + \varepsilon b a_s^\dagger \quad (17)$$

and their hermitian conjugates, where $\Delta_s = \Delta_a + \Omega_{\text{offs}}$ and $\Delta_i = \Delta_a - \Omega_{\text{offs}}$ are the detunings of the signal and idler fields when the frequency offset of the injected field from the fundamental frequency is Ω_{offs} . Because the control bandwidth is small compared to the cavity linewidth, we find the response of the error signals to a static change by setting the derivatives to zero and solving the set of equations. The input output relations can be used to find the coherent control fields in reflection off the OPO, $A_{s,r}, A_{i,r}$ and transmitted towards the interferometer, $A_{s,t}, A_{i,t}$:

$$A_{s,r} = \sqrt{2\gamma_a^c} a_s - A_{s,\text{in}} \quad A_{i,r} = \sqrt{2\gamma_a^c} a_i \quad (18)$$

$$A_{s,t} = \sqrt{2\gamma_a^f} a_s \quad A_{i,t} = \sqrt{2\gamma_a^f} a_i \quad (19)$$

The error signal in reflection off of the cavity (demodulated at twice the frequency offset of the injected field from the interferometer with a demodulation phase ϕ_{dm1} is proportional to:

$$E_r = \text{Re}[A_{s,r} A_{i,r}^\dagger] \sin \phi_{\text{dm1}} + \text{Im}[A_{s,r} A_{i,r}^\dagger] \cos \phi_{\text{dm1}} \quad (20)$$

In transmission the beat note with the local oscillator (A_{LO}) is demodulated at the offset frequency with a demodulation phase ϕ_{dm2} to give a signal proportional to:

$$E_t = \text{Re}[A_{s,t} A_{\text{LO}}^\dagger + A_{i,t}^\dagger A_{\text{LO}}] \sin \phi_{\text{dm2}} + \text{Im}[A_{s,t} A_{\text{LO}}^\dagger + A_{i,t}^\dagger A_{\text{LO}}] \cos \phi_{\text{dm1}} \quad (21)$$

The relative phase between the main squeezing laser and the coherent sideband injected into the OPO is adjusted to zero the reflected (coherent field) error signal, so the impact of fluctuations can be found by setting the error signal to zero and solving numerically for change in the phase of $A_{s,\text{in}}$. This phase is then propagated to the transmitted (quadrature control) error signal, and the shift of the pump phase required to zero this error signal gives the response of the entire coherent quadrature control scheme to a disturbance. The response of this scheme is the same as the response of the quadrature angle itself to fluctuations of the second harmonic pump phase, local oscillator phase, or path length from the OPO to the detector; this is a good control scheme to use to correct for fluctuations from those sources. Temperature and length fluctuations give rise to lock point errors in this control scheme.

Acknowledgments

The authors would like to thank the staff at LIGO Hanford Observatory for facilitating this experiment, especially Richard McCarthy, Filiberto Clara, and Dave Barker. We would also like to thank Valery Frolov, Hartmut Grote, Kate Dooley and Henning Valhbruch for valuable conversations and Melodie Kao, Raphael Cervantez, and Arati Prakash for their work on the experiment. LIGO was constructed by the California Institute of Technology and Massachusetts Institute of Technology with funding from the National Science Foundation and operates under cooperative agreement PHY-0757058. This paper has the LIGO document number LIGO-P1300068.